

X-641-65-451

NASA TM X-55395

# PARTICLE TRAJECTORIES IN MODEL CURRENT SHEETS

## 2. ANALYTICAL AND NUMERICAL APPLICATIONS TO AURORAS USING A GEOMAGNETIC TAIL MODEL

BY  
T. W. SPEISER

GPO PRICE \$ \_\_\_\_\_

CFSTI PRICE(S) \$ \_\_\_\_\_

Hard copy (HC) 3.00

Microfiche (MF) .50

FACILITY FORM 602

N66-17233  
(ACCESSION NUMBER)

(THRU)

52  
(PAGES)

(CODE)

13  
(CATEGORY)

(NASA CR OR TMX OR AD NUMBER)

(CATEGORY)

# 653 July 65

NOVEMBER 1965



**GODDARD SPACE FLIGHT CENTER**  
**GREENBELT, MARYLAND**

Presented in part at the Forty-Sixth annual meeting of the American Geophysical Union, P163a, Washington, D. C., April 22, 1965, and in part at the Ninth International Conference on Cosmic Rays, London, England, September, 1965.

Submitted to the Journal of Geophysical Research

Particle Trajectories in Model Current Sheets

2. Analytical and Numerical Applications  
to Auroras Using a Geomagnetic Tail Model<sup>†</sup>

T. W. Speiser<sup>1</sup>

Laboratory for Theoretical Studies

NASA, Goddard Space Flight Center

Greenbelt, Maryland

<sup>†</sup> Presented in part at the Forty-Sixth annual meeting of the American Geophysical Union, P163a, Washington, D. C., April 22, 1965, and in part at the Ninth International Conference on Cosmic Rays, London, England, September, 1965.

<sup>1</sup> National Academy of Sciences-National Research Council Resident Research Associate

Abstract. Individual particle trajectories are solved for in three models of possible field configurations of the geomagnetic tail. The analytical results of part 1 [Speiser, 1965b] are applied to two models. Both models contain magnetic field lines oppositely directed on either side of a neutral sheet, with an electric field perpendicular to the magnetic field and parallel to the neutral sheet. The models differ in the rate of variation of a magnetic field component perpendicular to the neutral sheet, and hence in the rate of field-line-crossing of the neutral sheet. For the two models, particles are accelerated and turned toward the earth within the neutral sheet and are ejected from the neutral sheet with small pitch angles to a magnetic line of force, with energies of tens-of-kilovolts. For the first model, a dipole-plus-tail model, electrons are ejected at about  $150 R_e$  and protons about  $50 R_e$  back in the tail. For the second model, an extended-tail-model, electrons are ejected at about  $500 R_e$ , and protons at about  $400 R_e$ . Proton auroras would be expected about  $1/2^\circ$  lower latitude than electron auroras, and isotropic fluxes should be measurable out to distances of the order of  $2.5 R_e$  from the earth. Extremely thin sheets of incoming particles are produced, about 1 km for electrons between 1 and 10 kev. The third model consists of a three-dimensional dipole field added to a tail/neutral-sheet field, and trajectories are calculated numerically, finding spatial regions of high intensity using Liouville's theorem. These spatially intense regions are near the auroral zones when mapped

onto the earth; they move to lower latitudes on the earth with an increase in the strength of the tail field, and their thickness is roughly proportional to the thermal velocity of the particles incident on the tail. The models may be applicable to other situations where neutral points or sheets may exist, such as the day-side magnetospheric current sheet, the interplanetary field, solar flares, etc.

Introduction. This paper is concerned with the possibility that the geomagnetic tail and more specifically, the neutral sheet in the tail, accelerates particles from the solar wind and is the immediate source of auroral particles.

Parker [1957] has investigated particle motion about a neutral sheet, and has found that regardless of the initial particle configuration, stability soon results with the current given by curl  $\underline{B}$ , just as in classical hydromagnetics. Weiss and Wild [1964], and Chapman and Kendall [1964] have also looked at particle trajectories about a neutral line without assuming the existence of any electric fields.

An essential part of Dungey's theory, however, concerns an electric field. He showed [Dungey, 1958] that if one assumes infinite conductivity at a neutral point, an infinite discharge develops in a finite time. Any finite conductivity would therefore limit the discharge and an electric field across the neutral region would remain. Such an electric field would be consistent with the "frozen-in" field of the advancing plasma.

Akasofu and Chapman [1961] developed a neutral line discharge theory of auroras, which is based upon one or more ring currents and with which they also hoped to explain the main phase of magnetic storms. Although this work was specifically pointed toward the ring current formation of neutral lines, later they suggest [Akasofu and Chapman, 1964] that the ring current is just one of the qualified sources of neutral lines and that in the general

sense, "the field line projection of an arc in the ionosphere on the equatorial plane must be a 'singular' line in the sense that on the line the guiding center approximation breaks down."

Piddington [1960] suggested that if some field lines from the earth were trapped into the solar wind at the time of a geomagnetic storm, a geomagnetic tail would be formed. His suggestion was made primarily to explain the main phase of geomagnetic storms, but he also mentioned that it might have "incidental effects" including auroral and Van Allen radiation, the gegenschein, and the diurnal variation of cosmic rays.

The neutral sheet in the geomagnetic tail has been probed with the Imp-1 satellite [Ness, 1965]. The sheet is about  $0.1 R_e$  (Earth-radii) thick and extends from about  $10 R_e$  to at least  $30 R_e$  (the apogee of Imp-1), and is found on almost every pass through the tail. Cahill's [1964] results using data from Explorer XIV complement Ness' results and show the tail structure in closer to the earth. These results generally fit the pattern of dipole field lines being stretched out in the tail and reversing across a neutral sheet beginning somewhere around  $10 R_e$ .

McDiarmid and Burrows [1965] using data from the Alouette 1 satellite at 1000 km, show occasional spikes of high intensity electrons (energies above 40 keV, fluxes approaching  $10^9 \text{cm}^{-2} \text{sec}^{-1} \text{ster}^{-1}$ ) occurring in a narrow latitudinal range at latitudes above the

trapping region. These field lines are therefore presumably connected to the tail and the tail is the source of the particles. Many other particle measurements in the tail show regions, usually near the neutral sheet, where the electron temperature is high, particle densities are much higher than interplanetary values, and intense fluxes or "islands" of energetic electrons are seen. [See Anderson, et al., 1965; Anderson, 1965; Frank, 1965; Gringauz, et al., 1960; Howard, et al., 1965].

If the magnetic field,  $B$ , at the center of the neutral sheet goes to zero, the gyro-radius increases without bound, so no matter how slowly  $B$  may vary,  $R/L$  ( $L$ , a characteristic system length) will be large, and adiabatic theory cannot be used. Particle trajectories must therefore be either solved for analytically from the equations of motion or computed numerically. If  $B$  is small but non-zero at the center of the sheet,  $R/L$  must be determined to see if adiabatic theory can be used.

In the following section, particle trajectories are calculated applying the results of the non-adiabatic analytic theory [Speiser, Part 1, 1965], (hereafter referred to as S1), to two models of the fields expected in the geomagnetic tail. A section follows where numerical trajectory results are given for a more complicated magnetic field geometry.

Analytical Applications. Although the geomagnetic tail has been probed, and magnetic field measurements have been made by Cahill [1964] out to about  $12 R_e$  and by Ness [1965] out to about  $30 R_e$ , measurements have not been made further back, and the exact description of the magnetic field inside the neutral sheet is not known. (An exception is the null result of Mariner IV [Coleman et al., 1965] where the geomagnetic tail was not found at  $3300 R_e$ .) A simple model of the fields in the geomagnetic tail will be assumed as indicated in Figure 1.

The electric field is taken to be uniform and across the tail (in the  $-\hat{e}_z$  direction of Figure 1). Such an electric field is based upon the flow patterns of the open model, [Dungey, 1961; 1958] and the work of Axford and Hines [1961], Axford, Petschek and Siscoe [1965], and Petschek [1964], and on ground observations of high latitude magnetic field fluctuations and their inferred current and equipotential systems. If an electric field does exist across the tail, it would most certainly have time and spatial dependencies. Such variations are not included in this model, but would modulate the results presented here. Measurements of electric fields in the magnetospheric tail have yet to be made, hence questions as to their existence are argumentative.

Using the fields of Figure 1, the results of S1 can be used. Those results are summarized as follows.



1. Particles of either sign incident on the neutral sheet oscillate about the sheet due to the reversal of the magnetic field.

2. As a particle oscillates about the sheet, it gains energy from the electric field, and is turned into the  $-\hat{e}_y$  direction (toward the earth) by  $B_x$ .

3. A particle will oscillate until it has been turned so much by  $B_x$  that  $\dot{z}$ , its velocity in the  $\hat{e}_z$  direction, changes sign. At that time the particle is ejected from the neutral sheet. (The ejection time is  $\tau = \pi/(q/m)b\eta$ .)

4. The velocity at ejection is almost entirely in the  $-\hat{e}_y$  direction if  $\eta \ll 1$ . (The ejection velocity  $\dot{y}(\tau) = -2a/\eta b$ .) Thus the ejection pitch angle ( $\alpha$ ) will be small if  $\eta$  is small. ( $\alpha \approx \eta/2 |\dot{x}_0/(a/b) - 2|$ .)

5. In the moving system where the electric field is transformed away, the motion is seen as an oscillation in  $x$  about the neutral sheet combined with a circular drifting of the trajectory in the neutral sheet (the  $y$ - $z$  plane). The neutral sheet effectively uncouples the circular drift from the oscillation about the sheet. (Although the oscillation is coupled to the circular drift.)

The electric field strength in the tail, "a", is assumed to be about 0.3 volts/km. This gives a potential of about 70 kilovolts across a tail of  $40 R_e$  diameter. This seems to be the right order of magnitude for the potential across the polar cap, which is mapped into the tail, assuming magnetic lines of force are equipotentials. Since particles gain energy by drifting across the tail while oscillating about the neutral sheet (item 2 above), an electric

field of different magnitude will affect the ejection velocity (item 4 above), and will limit the maximum attainable particle energy.

The magnetic field strength, "b", is taken to be  $20\gamma$  ( $1\gamma = 10^{-5}$  gauss =  $10^{-9}$  weber/m<sup>2</sup>). Ness [1965] finds the field to be from  $10$  to  $30\gamma$ , and about  $40\gamma$  at the time of a magnetic storm.

The other parameter,  $\eta$ , that we need to know is the ratio of the magnetic field component perpendicular to the neutral sheet,  $B_x$ , to "b", the solar-antisolar field strength outside of the neutral sheet. As a first case, we will assume that  $B_x$  is furnished by the earth's dipole field as sketched schematically in Figure 1. This assumption is certainly artificial and merely provides a model for the rate of crossing of field lines through the neutral sheet. Using such a model implies that the field strength at the center of the neutral sheet at  $16 R_e$  is about  $7\gamma$ , and this seems to be larger than that measured by Ness [p. 2993, Figure 3, 1965]. Another model for  $B_x$  is discussed at the end of this section.

Referring to Figure 1 for the values of the constants, and using the results of S1, Table 1 can be constructed. Figure 2 shows a sketch of particle trajectories for this model.

Particle enters the neutral sheet in the tail at:	$\eta$ $B_x$ (dipole) $(= \frac{\quad}{b})$	Proton energy at ejection	Electron energy at ejection	$y_p(\tau)$ Distance protons travel towards the earth before ejection	$y_e(\tau)$ Distance electrons travel towards the earth before ejection	$z_p(\tau)$ Distance protons travel across the tail before ejection	$z_e(\tau)$ Distance electrons travel across the tail before ejection	$\alpha$ Maximum pitch angle of particles at ejection
50 $R_e$	$1.25 \times 10^{-2}$ ( $B_x = \frac{1}{4} \gamma$ )	30 kev	16 ev	-25 $R_e$	- 80 km	-16 $R_e$	50 km	$0.4^\circ$ + $4^\circ$ #
150 $R_e$	$4.63 \times 10^{-4}$ ( $B_x = 10^{-2} \gamma$ )	70 kev (Maximum potential across the tail)	12 kev	Protons drift completely across the tail	-10 $R_e$	Protons drift completely across the tail	6 $R_e$	$0.01^\circ$ + $.1^\circ$ # $5^\circ$ #

a=0.3 volts/km, b=20  $\gamma$

+ Assuming  $|\frac{\dot{x}_0}{u} - 2| = 1$

# Assuming  $|\frac{\dot{x}_0}{u} - 2| = 10$

# Assuming  $|\frac{\dot{x}_0}{u} - 2| = 400$

Table 1

The analytical study (S1) was based on the assumption that  $\eta$  is a constant. From Table 1, for protons at  $50 R_e$ , it is seen that the particle drifts  $25 R_e$  toward the earth before it is ejected from the sheet. Using the dipole model,  $\eta$  would change by a factor of eight, so the above-mentioned approximation does not seem very good. The larger  $\eta$  would serve to turn the proton in a tighter circle, and the proton would be ejected sooner and would gain less energy than indicated in the table. However, if a trajectory is broken into a number of small segments, over each of which  $\eta$  is approximately a constant, then S1 can be used over each segment. For the above example, when the proton has drifted in to about  $40 R_e$ , it has already gained about 20 kev, so the inconstancy of  $\eta$  does not affect the results as much as would be at first supposed. This is because the biggest part of the energy gain is during the first part of the trajectory before the particle has been turned much in toward the earth.

In S1 the qualitative behavior of the oscillation about the neutral sheet has been determined, but the details have not been solved for analytically. Knowledge of the output pitch angle requires the detailed knowledge of all of the velocity components at output.  $\dot{x}$  was estimated as of the order of  $\dot{x}_0$ , and  $\dot{z}$  was estimated as of the order of zero, since ejection occurs when  $\dot{z}$  changes sign. The pitch angles in Table 1 are therefore shown for several values of  $\dot{x}_0$ , making the above assumptions.

Many proton trajectories have been computed, solving the equations of motion using a Runge-Kutta computer subroutine. Using  $B_x = 1/4\gamma$  (from the earth's dipole field at  $50 R_e$ ) and the values of "a" and "b" as used in Table 1, it is found that ejection pitch angles lie between 0 and 6 degrees for incoming velocities of zero to 200 km/sec.

From Table 1, at  $50 R_e$  if  $\dot{x}_0 \approx 12u \approx 200$  km/sec, a pitch angle of about  $4^\circ$  is expected, and is therefore in general agreement with the computed value. However, the computations do not show the pitch angle to be related to  $\dot{x}_0$  in as simple a manner as found from the qualitative arguments for determining the pitch angle of S1 (paragraph 4. above).

The analysis (S1) of the energy gained, the turning of the trajectory toward the earth, the trapping in the neutral sheet and subsequent ejection when  $\dot{z}$  changes sign are all confirmed by the trajectory computations. The qualitative behavior, oscillation frequency, amplitude variation, etc., about the neutral sheet also agrees with the theory. At ejection, however, the perpendicular velocity components  $\dot{x}$  and  $\dot{z}$ , and hence the pitch angle, depends on where the particle is and what its velocity is when  $\dot{z}$  changes sign. If the particle is close to the peak of its last oscillation when  $\dot{z}$  changes sign, it will have a small  $\dot{x}$  and thus small pitch angle; if it is close to  $x = 0$ , its  $\dot{x}$  will be large and will increase until ejection, and will thus imply a large pitch angle.

Figure 3 is a machine computation of a proton trajectory using the fields of Figure 1 and the constants as in Table 1. The initial velocities at the neutral sheet ( $x = 600$  km) are indicated. The comparisons of the theoretical (Sl) predictions with the computed values are indicated on Figure 3.

Dungey [1965] predicts a tail length of the order of  $1000 R_e$ , so a neutral point may exist at about  $500 R_e$ . A possible model for the perpendicular component,  $B_x$ , would therefore be one which goes linearly from about  $1\gamma$  at about  $50 R_e$  to zero at  $500 R_e$ . This model is sketched in Figure 4. The limiting field line from the neutral point as sketched is attached to the auroral zone in agreement with Dungey's [1961] open model. Table 1 can be used for the application of the analytical results to this model, with the only modification being the first entry, that is the distance back in the tail at which the particle enters the neutral sheet. For the first column  $B_x$  is  $1/4\gamma$  at  $y = 388 R_e$ , so protons of about 30 kev will come from this region, and electrons of about 12 kev energy will come from the region where  $B_x \approx 10^{-2}\gamma$  or from about  $495 R_e$ .

From conservation of flux we can find the latitudinal separation at the earth of the two field lines which come from  $388 R_e$  and  $495 R_e$ . That is:

$$\int_{\text{earth}} \underline{B} \cdot d\underline{A} = \int_{\text{tail}} \underline{B} \cdot d\underline{A}, \quad \text{or} \quad (1)$$

$$B_0 R_e^2 \int_{23^\circ}^{\theta_1} \sin\theta \, d\theta = \int_{386 R_e}^{495 R_e} B_x(y) T \, dy \quad (2)$$

where  $B_0 \approx 60,000\gamma$  (assumed constant if  $\theta_1$  is small),  $B_x(y)$  is taken from Figure 4, and  $T$ , the tail width, is assumed about  $40 R_e$ . For the above example,  $\theta_1$  comes out to be about  $23.4^\circ$ ; thus for this model of the fields, protons are ejected along field lines which intersect the earth's surface about  $0.4^\circ$  lower latitude than do the field lines along which energetic electrons are ejected.

From the analytic study, Sl, it was found that the velocity of the particles ejected from the neutral sheet varies inversely as  $B_x^2$ . For electrons, the relationship is therefore

$$W = (1.2/B_x^2)$$

where  $W$  is the energy in eV, and  $B_x$  is in gammas. For the model used in Figure 4, we have

$$B_x = \frac{500 \cdot y}{450} \gamma \quad (3)$$

with  $y$  measured in earth-radii ( $R_e$ ). Therefore the ejected electron energy as a function of distance back in the tail is

$$W = \frac{2.4 \times 10^5 \text{ eV}}{(500-y)^2}, \quad (4)$$

and the equivalent proton energy is found by multiplying the right-hand side of equation (4) by 1,836. Both expressions for the energy are valid until the maximum potential across the tail has been gained (see Table 1). The co-latitude is found as a function of distance in the tail by conserving flux as before, and from equation (4), the electron energy can be found as a function of co-latitude, and this is:

$$\theta - \theta_0 = \frac{0.14}{W} \quad (5)$$



where the angles are in radians for  $W$  in eV, and  $\theta_0 = 23^\circ$ . From equation (5) the latitudinal separation on the earth for ejected electrons from 1 keV to 10 keV, for example, is found to be about  $1.3 \times 10^{-4}$  radians, which corresponds to a beam width of about 0.8 km thickness at the earth.

M. P. Nakada [private communication, 1965] has suggested that field line loading may be an important problem for any auroral theory in which the particle source is located far away. That is, fluxes of particles with energies and intensities large enough for auroras may have more energy density than magnetic field energy density if they come from weak regions of magnetic field, and if these fluxes are isotropic in the weak-field-region.

O'Brien [1964] observed that the average energy flux of electrons with energies greater than 1 keV precipitated in the auroral zone is about  $4 \text{ ergs cm}^{-2} \text{ sec}^{-1}$ . He also notes that fluxes may occasionally be as high as  $2000 \text{ ergs cm}^{-2} \text{ sec}^{-1}$ , [McIlwain, 1960; O'Brien and Laughlin, 1962]. Assuming these fluxes are of 10 keV electrons, the above numbers imply fluxes of  $3 \times 10^8$  to  $1.5 \times 10^{11}$  electrons  $\text{cm}^{-2} \text{ sec}^{-1}$ , and thus densities of .05 to 25 electrons  $\text{cm}^{-3}$ . Omholt [1963] estimates densities as high as 1000 electrons  $\text{cm}^{-3}$  at the time of an intense aurora.

To see what sort of densities this implies for a source, assume for the region between the source and the earth Liouville's theorem holds; energy is conserved (after ejection for the model S1);  $\mu$ , the

first adiabatic invariant is conserved. Liouville's theorem allows us to write

$$f = \frac{J}{E} \text{ (particles cm}^{-2} \text{ sec}^{-1} \text{ ster}^{-1} \text{ energy}^{-1}\text{)} = \text{constant} \quad (6)$$

which implies  $J = \text{constant}$  from the second assumption above. The number density  $N$ , (particles  $\text{cm}^{-3}$ ) is found by integrating  $Jv^{-1}$  ( $v$  is the particle velocity) over solid angle and energy. In this example it will be assumed that  $J$  is independent of the solid angle  $\Omega$ , (the flux is isotropic), and exists for only one energy (the flux is monochromatic). Then, at the earth,

$$N_e = \int \frac{J_e \delta(E_e - E_0) d\Omega_e dE_e}{\left(\frac{2E_e}{m}\right)^{\frac{1}{2}}} = \frac{2\pi J_e}{\left(\frac{2E_0}{m}\right)^{\frac{1}{2}}} \quad (7)$$

where the subscript  $e$  refers to the earth. In the tail (subscript  $t$ ) we have

$$N_t = \int \frac{J_t \delta(E_t - E_0) d\Omega_t dE_t}{\left(\frac{2E_t}{m}\right)^{\frac{1}{2}}} = \frac{J_e}{\left(\frac{2E_0}{m}\right)^{\frac{1}{2}}} \int \frac{d\Omega_t}{d\Omega_e} d\Omega_e \quad (8)$$

where use has been made of Liouville's theorem. To evaluate  $N_t$ , we use the conservation of  $\mu$  and  $E$  to obtain:

$$\frac{\sin^2 \alpha_e}{B_e} = \frac{\sin^2 \alpha_t}{B_t} \quad (9)$$

along with the definition of solid angle

$$d\Omega_t = 2\pi \sin \alpha_t d\alpha_t \quad (10)$$

$$d\Omega_e = 2\pi \sin \alpha_e d\alpha_e$$

where  $\alpha$  is the particle pitch angle. Therefore,

$$\frac{d\Omega_t}{d\Omega_e} = \frac{B_t}{B_e} \frac{\cos \alpha_e}{\sqrt{1 - B_t B_e^{-1} \sin^2 \alpha_e}} \quad (11)$$

and, evaluating the integral,

$$N_t = \frac{2\pi J_e}{(2E_0/m)^{\frac{1}{2}}} (1 - \sqrt{1 - B_t B_e^{-1}}) \quad (12)$$

so

$$\frac{N_t}{N_e} = (1 - \sqrt{1 - B_t/B_e}) \quad (13)$$

or

$$\frac{N_t}{N_e} = \frac{1}{2} B_t/B_e \quad \text{for } B_t \ll B_e. \quad (14)$$

If we now equate particle energy density in the tail to magnetic energy density, we have

$$E_0 N_t = 2.65 B_t^2 \quad (15)$$

for  $E_0$  in eV, and  $B_t$  in gammas, and using equation (14) we have

$$B_t = \frac{E_0}{5.3} \frac{N_e}{B_e} \quad (16)$$

or, for  $E_0 = 10$  kev, and  $B_e = 60,000\gamma$ ,

$$B_t = \frac{N_e}{32} \quad (17)$$

Thus to have the same energy density in the field as in the particles for O'Brien's  $2000 \text{ ergs cm}^{-2} \text{ sec}^{-1}$  ( $N_e = 25 \text{ electrons cm}^{-3}$ ) requires a tail field of only about  $1\gamma$ . If Omholt's estimate of  $N_e \approx 1000$  electrons  $\text{cm}^{-3}$  is at times correct, a tail field of about  $30\gamma$  would have about the same energy density as particle energy density. If we make the further assumption that the particle energy density be at most 10% of the tail magnetic energy density, then tail fields of 10 to  $300\gamma$  are required. If, however, auroral particles are shot nearly along magnetic lines of force from the source, as they are from the mechanism reported in this paper, then the pressure perpendicular to magnetic lines of force, tending to push field lines out can be much smaller than the isotropic case. Therefore a smaller  $B_t$  can contain the particles.

Discussion of Analytical Applications. The significant results of the previous applications of the analytic theory (S1) to a tail model of the earth are that particles are accelerated, turned in toward the earth and ejected from the neutral sheet with small pitch angles to the magnetic lines of force. This ejection at small pitch angles may be important for the prevention of "field line loading" as discussed in the previous section. Certainly more experimental observations on particle fluxes and energies and magnetic field configurations are needed before some of these questions can be answered.

These applications also predict proton auroras to be at lower latitudes than electron auroras, (for the second model the latitudinal separation is about  $0.4^\circ$ ). Omholt [1963] says "There is often (perhaps always) a distinct dark region (up to  $1^\circ$  in latitude) between the 'proton aurora' and the main forms."

Electrons in the energy range from 1 to 10 kev would be found in an extremely thin beam at the earth, i.e. about one kilometer thickness. Equation (5) also predicts a hardening of the beam with latitude, but the electric drift between the ejection point and the earth has been neglected, (this would tend to move the higher energies to slightly lower latitudes), and the self-consistency of such a thin beam has not been investigated. This result may therefore be incorrect.

The analytic results also predict a monochromatic beam at a given point in space, but those results are approximate and based on the assumption that the perpendicular component of magnetic field in the neutral sheet,  $B_x$ , is constant. For a linear variation of  $B_x$  as used here, a different spectrum should be found, but this requires computing, and has not yet been done.

O'Brien [1964] suggests that a major experimental study should be made to determine the limits of isotropy in the incident beam and thus the cause of auroral precipitation. He finds that for electrons with energies greater than 40 kev, fluxes are isotropic to within 10% at 1000 km. The results of the present study imply fluxes from the tail within a cone of the order of 0.1 radian, and thus one would expect to measure isotropic fluxes out to about 2.5 earth-radii.

The difference between the second model used, (as in Figure 4), and the dipole-plus-tail model lies in the distance from the earth at which particles are ejected from the neutral sheet. Indeed, any model giving a different variation of  $B_x$  (hence a different rate of crossing of field lines through the neutral sheet) will merely move the particle ejection points toward or away from the earth. If, however,  $B_x$  is negative, then particles will be turned away from the earth and will be ejected into the tail (in the anti-solar direction). Close to the earth, however,  $B_x$  is positive, so it is

likely that it becomes very weak far from the earth, and it would reverse if there is a neutral point somewhere in the tail. Such a reversal is likely if the interplanetary field has a southward component and the field has to eventually fit onto the interplanetary field. Thus, if there is a neutral point in the tail as indicated in Figure 4, and if the electric field is as indicated, particles will be shot in toward the earth between the earth and the neutral point, and will be shot away from the earth on the other side of the neutral point.

If the electric field in the tail is radial as Taylor and Hones [1965] suggest, then this mechanism can work over the dusk half of the tail (meaning negative values of  $z$ ), but will not work over the dawn half (positive  $z$ ). Their electric field is in the  $+\hat{e}_z$  direction for the dawn half of the tail, and particles will not be trapped in the sheet in this region. However, the bulk flow velocity or circulation is such as to bring particles into the dusk half for their model.

For particles to be trapped in the neutral sheet, it is only necessary that the magnetic field reverse across the sheet so that the magnetic force term in the Lorentz-force equation reverses across the sheet. The specific linear variation used in S1 lends itself to analytic solution and is probably valid over some portion of the sheet.



The self-consistent problem has not been solved. However, one interesting result of S1 and these applications is that particles of different masses injected at the same point on the neutral sheet are trapped, accelerated, turned, and all are ejected with the same velocity. So from this simple viewpoint, space charges should not build up to invalidate the mechanism. This, however, assumes a neutral sheet of infinite extent, and is probably correct over the regions where the protons are turned and ejected toward the earth with energies in the tens of kilovolts. But in the region where the electrons are ejected with the same energies, protons drift completely across the tail, and thus leave the sheet (when the maximum potential has been gained) with smaller velocities than the electrons. Space charges may thus build up in this regime, limiting the electric field. Whether or not this is a real problem must await a self-consistent analysis.

Numerical Solutions. Speiser [1965a], presented results of numerical solutions of particle trajectories about a model current sheet. The model used was chosen for the fields "guessed" in the geomagnetic tail, but no connection was made to field lines at the earth. Those results showed that accelerated protons, emergent along magnetic lines of force, have their greatest intensity in a thin output sheet. A similar study was not made for electrons because of the enormous amount of computer time involved, but on the basis of a few trajectories it was suggested that the spatial structure for electrons would be much thinner than that for protons. These results are substantiated by the analytical results in the previous section of this paper.

In order to make mappings of the output sheets onto the earth, a dipole-plus-tail model is used. This model is the same as that used for the analytical study in the previous section, but all of the components of the dipole magnetic field are kept, and not just  $B_x$  as in Figure 1. The method of procedure is the same as used before [Speiser, 1965a] and will only be summarized here.

1. A three dimensional dipole field is added to a tail field which is  $B_t$  as indicated in Figure 1. This field is certainly incorrect in the dayside magnetosphere and will only be used for calculations in the tail.

2. A proton trajectory is started at some point on an output plane ( $x_0$ - $z_0$  plane), with a velocity directly along the magnetic line of force through that point, and the trajectory is then

numerically solved backwards in time. After the particle has passed through the neutral sheet (backwards in time) its velocity on the input side is noted. Assuming a Maxwellian distribution, a value for the distribution function can then be found on the input side.

3. Using Liouville's theorem, the distribution function is constant along a trajectory; an intensity map over the output plane ( $x_0$ - $z_0$ ) may then be made.

4. Regions of greatest intensity may then be mapped onto the earth by solving for the trajectories forward in time from the output plane.

Figure 5 shows backwards plots for three protons, with only the x-component versus time. The strength of the tail field,  $b$ , is  $20\gamma$ , the y and z starting positions are  $y_0 = 26.5 R_e$ ,  $z_0 = 0.1 R_e$ , and  $v_0 = 1664$  km/sec for all trajectories. It is seen that if the particle starts with too large an  $x_0$ , it follows a field line back for a time, and then the electric drift causes the particle to drift away from the neutral sheet (backwards in time). Since the particle's energy changes only in the neutral sheet, its speed is the same on the input side ( $t \approx -170$  sec). A second particle starts at  $x_0 \approx 3000$  km, reaches the neutral sheet and oscillates about 16 times before input. Its energy has thus changed very much and the particle can have a small velocity at input. The remaining trajectory also reaches the neutral sheet, but does not stay in long before input ( $t \approx -50$  sec). Its energy has therefore not changed much, and its input velocity is not as small as the preceding particle. Using the ideas from S1, we can say that this latter particle did not stay so long in the neutral sheet because

$B_x$  was larger for it and the particle was ejected sooner than the preceding particle.

If one therefore expects the majority of particles incident on the neutral sheet to have small velocities, then the middle trajectory of Figure 5 should indicate the region of the largest output intensity, since particles with nearby trajectories come from highly populated regions of velocity space. This is a crude explanation of the use of Liouville's theorem, and of why such a model produces the largest intensities of output particles in thin sheets.

Writing the distribution function as

$$f = A e^{-F^2/v_t^2}$$

where  $F = v - u$ ,  $v$  is the particle velocity,  $u$  is the bulk flow velocity, and  $v_t$  is the thermal velocity, we can see that  $f$  is largest when  $F < v_t$ .

Figure 6 shows a contour map of  $F$  on the  $x_0$ - $z_0$  plane.  $F$  does reach lows of about "100 km/sec" in regions near the center of the "200 km/sec" contours, and the breaks in the "200 km/sec" contours are probably not real, i.e., they would probably disappear if a plot with a finer net were used.

Figure 7 shows the positions of the output sheets with large intensity ( $F < v_t$ , and  $v_t \approx 100$  km/sec) on the  $x_0$ - $z_0$  plane for various tail fields.

Figure 8 maps the intersections of Figure 7 forward onto the earth, using the dipole-plus-tail model.

Discussion of Numerical Results. These numerical calculations have only been done for protons using a three dimensional dipole-plus-tail model. The results show that the largest intensities of particles accelerated in the neutral sheet and coming out along magnetic lines of force occur in thin sheets. (If  $v_t$  is taken to be larger than 100 km/sec, from Figure 6, the thickness of the output sheets is increased.) These sheets when mapped onto the earth intersect the earth near the auroral zones, and the sheets move to lower latitudes with an increasing tail field. These results are for only one output velocity, 1664 km/sec corresponding to a proton energy of about 12 kev. A longitudinal assymetry would be expected for higher energy protons, in a plot like Figure 8, since the tail has only finite width, and the particles must drift across the tail in the neutral sheet to gain energy.

Figure 8 is not expected to be quantitatively accurate since the dipole-plus-tail model is not very good near the earth, and no good on the day-side. Williams and Mead [1965, page 3025, Fig. 6] develop a magnetic field model in the magnetosphere which utilizes the dipole field, the field due to magnetospheric surface currents, and a current sheet in the tail. Using their Figure 6, the field line passing through  $x_0 = 3000 \text{ km} \approx 1/2 R_e$ , at  $y_0 \approx 25 R_e$  comes from a latitude between  $65^\circ$  and  $70^\circ$ . Therefore, using their model for mapping the intersections of Figure 7 onto the earth would lower the mappings of Figure 8 by about  $5^\circ$ , which would be in better agreement with the auroral zones.

Summary and Conclusions. A simple model is used for the possible electric and magnetic field configuration in the tail of the earth's magnetosphere. Satellite measurements out to about  $30 R_e$  have shown the general result of high latitude field lines being pulled back in the tail, with the formation of a neutral-or current-sheet across which the field reverses direction. Not much is known yet about the field at the center of this neutral sheet, or about the existence of any electric fields. For the models discussed here, an electric field across the tail generally from dawn to dusk is assumed to exist, and a weak magnetic field component perpendicular to the neutral sheet and tending toward zero with distance is assumed inside the neutral sheet. These features need not be permanent, but can cause particle trapping and acceleration in the neutral sheet whenever they may exist. The self-consistency of these solutions and the effects of various instabilities should be investigated but this has not yet been done.

Two models, a dipole-plus-tail model (Figure 1) and an extended tail model (Figure 4) are used to apply the analytic theory (S1). In both cases, electrons and protons incident on the neutral sheet are trapped, accelerated, turned toward the earth, and ejected from the neutral sheet with small pitch angles to a magnetic line of force. The main difference between the two models is the ejection point back in the tail. For the two models electrons of the order of 10 keV are ejected at about  $150 R_e$  and  $500 R_e$  respectively, and for protons of about 30 keV, the ejection distances are about  $30 R_e$  and

$400 R_e$ , respectively. The model produces extremely thin beams of incoming particles at the earth, about 1 km for electrons between 1 and 10 kev. Proton auroras are produced at latitudes about  $1/2^\circ$  lower than electrons, and isotropic fluxes should be expected out to about  $2.5 R_e$ .

Many trajectories of about 12 kev protons have been computed for a three-dimensional dipole-plus-tail model. Using Liouville's theorem, regions of large intensity are found which are near the auroral zones when mapped onto the earth. An increase of the tail field moves the mapping onto the earth to lower latitudes.

These features agree generally with some auroral observations, namely: the latitude of the auroral zones; the energies of auroral protons and electrons; the fluxes of auroral protons and electrons; the appearance of proton auroras at lower latitudes than electron auroras; a dawn/dusk assymetry for electron/proton auroras; the movement of auroral forms to lower latitudes with an increasing tail field (hence solar wind pressure); the thinness of auroral forms; and the gross conjugacy of auroral events.

The models may be applicable to other situations where neutral-points or sheets are thought to exist, such as the day-side magnetospheric current sheet, neutral points in the interplanetary field, the influence of Jupiter's satellite Io on Jupiter's radio emission [Warwick and Dulk, 1965], and solar flares. Since the models predict particles accelerated and ejected with the same velocity independent of mass, a comparison could be made, for example,



of helium and proton energies in a flare (or in the geomagnetic tail) to see if they are in the ratio of the masses. If some of the recently observed "red spots" on the moon [Kozyrev, 1959; 1963; Greenacre, 1963; Cameron, 1965] are due to fluorescence, the particles could come from this mechanism while the moon is in or near the earth's tail.

## REFERENCES

- Akasofu, S. -I., and S. Chapman, A neutral line discharge theory of the aurora polaris, Phil. Trans., 253, 359, April 27, 1961.
- Akasofu, S. -I., and S. Chapman, Magnetic storms and auroras, Ch.
- Anderson, K. A., Energetic electron fluxes in the tail of the geomagnetic field, J. Geophys. Res., 70 (19), 4741, Oct. 1, 1965.
- Anderson, K. A., H. K. Harris and R. J. Paoli, Energetic electron fluxes in and beyond the earth's outer magnetosphere, J. Geophys. Res., 70, 1039, 1965.
- Axford, W. I., and C. O. Hines, A unifying theory of high-latitude geophysical phenomena and geomagnetic storms, Can. J. Phys., 39, 1433, 1961.
- Axford, W. I., H. E. Petschek and G. L. Siscoe, The tail of the magnetosphere, J. Geophys. Res., 70 (5), March 1, 1965.
- Cahill, L. J., Preliminary results of magnetic field measurements in the tail of the geomagnetic cavity, I. G. Bull., 79, Trans. Am. Geophys. Union, 45, 231, 1964.
- Cameron, W. S., A summary of lunar transients, to be published, 1965.
- Chapman, S., and P. C. Kendall, Non-adiabatic motion of charged particles traversing a weak magnetic field: pitch angle scattering, Pure and Appl. Geophys., 59, 100, 1964/III.

- Coleman, P. J., Jr., L. Davis, Jr., D. E. Jones, and E. J. Smith,  
Mariner 4 magnetometer observations (title only), Trans.  
Am. Geophys. Union, 46, 113, 1965.
- Dungey, J. W., Cosmic Electrodynamics, Cambridge Univ. Press,  
Cambridge, 1958.
- Dungey, J. W., Interplanetary magnetic field and the auroral zones,  
Phys. Rev. Letters, 6 (2), 47, Jan. 15, 1961.
- Frank, L. A., A survey of electrons beyond 5  $R_e$  with Explorer 14,  
J. Geophys. Res., 70, 1593, 1965.
- Greenacre, J. A., A recent observation of lunar color phenomena,  
Sky and Telescope, 26 (6), 316, Dec., 1963.
- Gringauz, K. I., V. G. Kurt, V. I. Moroz, and I. S. Shklovsky,  
Results of observations of charged particles observed out to  
100,000 km with the aid of charged particle traps on Soviet  
space probes, Astron. Zh., 37 (4), 716, 1960.
- Howard, H. T., V. R. Eshleman, G. H. Barry, and R. B. Fenwick,  
Radar measurements of the total cislunar electron content,  
J. Geophys. Res., 70 (17), 4357, Sept. 1, 1965.
- Kozyrev, N. A., Observation of a volcanic process on the moon,  
Sky and Telescope, 18, 184, 1959.
- Kozyrev, N. A., Volcanic phenomena on the moon, Nature, 198 (4884),  
979, 1963.
- McDiarmid, I. B., and J. R. Burrows, Electron fluxes at 1000 kilometers  
associated with the tail of the magnetosphere, J. Geophys. Res.,  
70 (13), 3031, July 1, 1965.

- McIlwain, C. E., Direct measurement of protons and electrons in visible aurorae, Space Research, Proc. Intern. Space Sci. Symp., 1st, Nice, 1960, ed. by H. K. Kallman-Bijl, pp. 715-720, North-Holland Publ. Co., Amsterdam, 1960.
- Ness, N. F., The earth's magnetic tail, J. Geophys. Res., 70, (13) 2989, July 1, 1965.
- O'Brien, B. J., High latitude geophysical studies, 3, J. Geophys. Res., 69, 13-43, 1964.
- O'Brien, B. J., and C. D. Laughlin, An extremely intense electron flux at 1000 km altitude in the auroral zone, J. Geophys. Res., 69 (1), Jan. 1, 1964.
- Omholt, A., Observation and experiments pertinent to auroral theories, Pl. and Sp. Sci., 10, 247, 1963.
- Parker, E. N., Newtonian development of the dynamical properties of ionized gases of low density, Phys. Rev., 107 (4), 924, August 15, 1957.
- Petschek, H. E., Magnetic field annihilation, in: AAS-NASA Symp. on the Physics of Solar Flares, ed. by W. N. Hess, Washington, D. C., NASA, (NASA SP-50), pp. 425-439, 1964.
- Piddington, J. H., Geomagnetic storm theory, J. Geophys. Res., 65 (1), 93, Jan., 1960.
- Speiser, T. W., Particle trajectories in model current sheets, 1. analytical solutions, J. Geophys. Res., 70 (17), 4219, Sept. 1, 1965 (S1).

Speiser, T. W., Particle trajectories in a model current sheet,  
based on the open model of the magnetosphere, with applications  
to auroral particles, J. Geophys. Res., 70 (7), 1717,  
April 1, 1965a.

Taylor, H. E., and E. W. Hones, Jr., Adiabatic motion of auroral  
particles in a model of the electric and magnetic fields  
surrounding the earth, J. Geophys. Res., 70 (15), 3605, 1965.

Warwick, J. W., and G. A. Dulk, Asymmetries, particles, and satellites  
in the magnetosphere of Jupiter, Trans. A. G. U., 46 (3),  
530, 1965.

Weiss, A. A., and J. P. Wild, The motion of charged particles in  
the vicinity of magnetic neutral planes with applications  
to type III solar bursts, Aust. J. of Phys., 17, (3), 282,  
Sept., 1964.

Williams, D. J., and G. D. Mead, Nightside magnetosphere configuration  
as obtained from trapped electrons at 1100 kilometers,  
J. Geophys. Res., 70 (13), 3017, July 1, 1965.

Acknowledgements. I am grateful for many discussions to Dr. M. P. Nakada, Dr. W. N. Hess, Dr. J. G. Roederer, Dr. T. G. Northrop, Dr. G. D. Mead, Dr. N. F. Ness, Mrs. W. S. Cameron, and am especially grateful to Prof. J. W. Dungey for many discussions and criticisms. I also wish to thank Mrs. E. H. Glover for assistance with some of the computer programs.

## FIGURE CAPTIONS

Figure 1. Dipole-plus-tail model (in the meridian plane containing the earth-sun line). The thickness of the neutral sheet is  $2d$ , the magnetic field strength outside the sheet is " $b$ ",  $B_x$  or " $\eta b$ " is determined from the dipole field at a particular location, and the electric field strength is " $a$ ". Arrows are magnetic field components.

Figure 2. Sketch of particle trajectories using the fields of Figure 1. Both protons and electrons oscillate about the sheet accelerating in opposite directions, and are turned in the same direction by the small magnetic field component perpendicular to the sheet. The direction turned is toward the earth if this perpendicular component is northward as indicated, otherwise into the tail if the component is southward. When the particles are turned  $90^\circ$ , they are ejected from the neutral sheet. Electrons come out much sooner than protons, with the same velocity as protons, hence gain less energy. The dimensions shown are illustrative and not to scale.

Figure 3. Isometric trajectory plot of a proton trajectory in the dipole-plus-tail model, see Figure 1,  $B_x = 1/4\gamma$ ,  $b = 20\gamma$ ,  $d = 600$  km,  $a = 1/3$  volt/km. For this model the earth would be at  $-50 R_e$ . Initial conditions;  $x = 600$  km,  $y = z = 0$ ,

$\dot{x} = -60$  km/sec,  $\dot{y} = 15$  km/sec,  $\dot{z} = 10$  km/sec.  $\tau$  is the ejection time,  $\alpha$  is the ejection pitch angle.

Figure 4. Extended tail model. Field lines are sketched for the above model, where  $B_x$  is assumed to vary as indicated, going from  $1\gamma$  at  $50 R_e$  to zero at  $500 R_e$ .

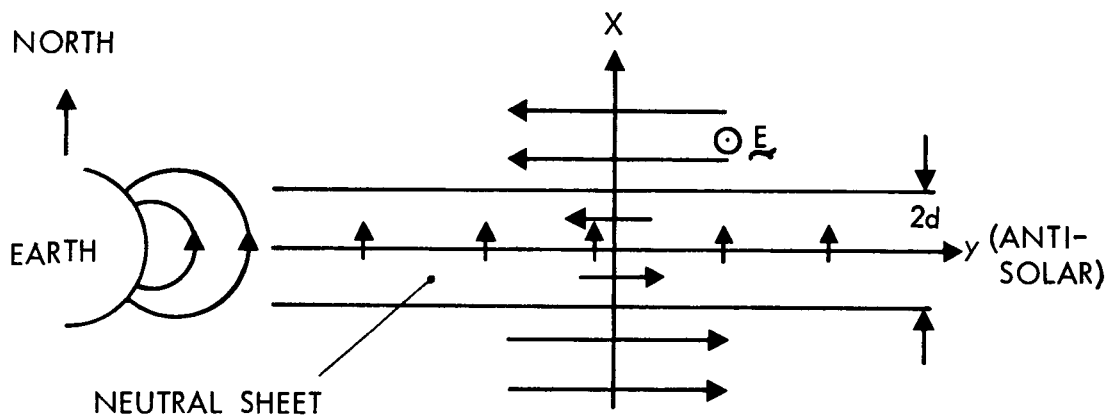
Figure 5. Backwards trajectory plots, starting at  $z_0 = 0.1 R_e$ ,  $y_0 = 26.5 R_e$ ,  $v_0 = 1664$  km/sec.

Figure 6. F contours in units of 200 km/sec,  $y_0 = 26.5 R_e$ .

Figure 7. Intersections of sheets with largest intensity with the  $x_0$ - $z_0$  plane ( $y_0 = 26.5 R_e$ ).

Figure 8. Mapping of intersections of Figure 7 onto the earth using the simple dipole-plus-tail model. These mappings move about  $5^\circ$  lower in latitude when Williams and Mead's [1965] field model is used. An asymmetry would be expected for higher energy particles, or for the same energy if the electric field were weaker, when a tail of finite width is considered. Protons would be shifted toward dusk and afternoon, and electrons would be shifted toward dawn and morning.



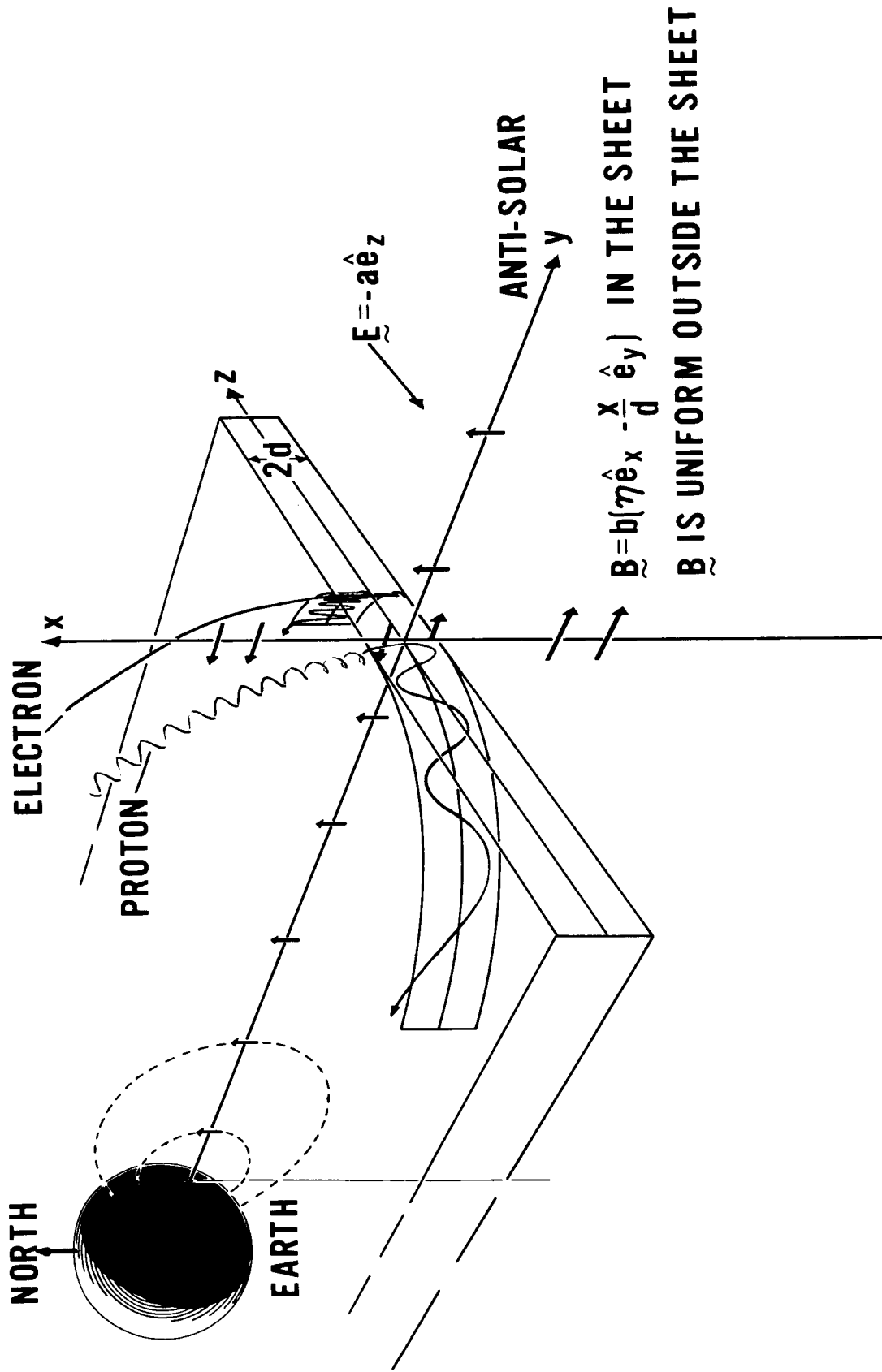


$$\vec{B} = B_x \hat{e}_x + \vec{B}_t$$

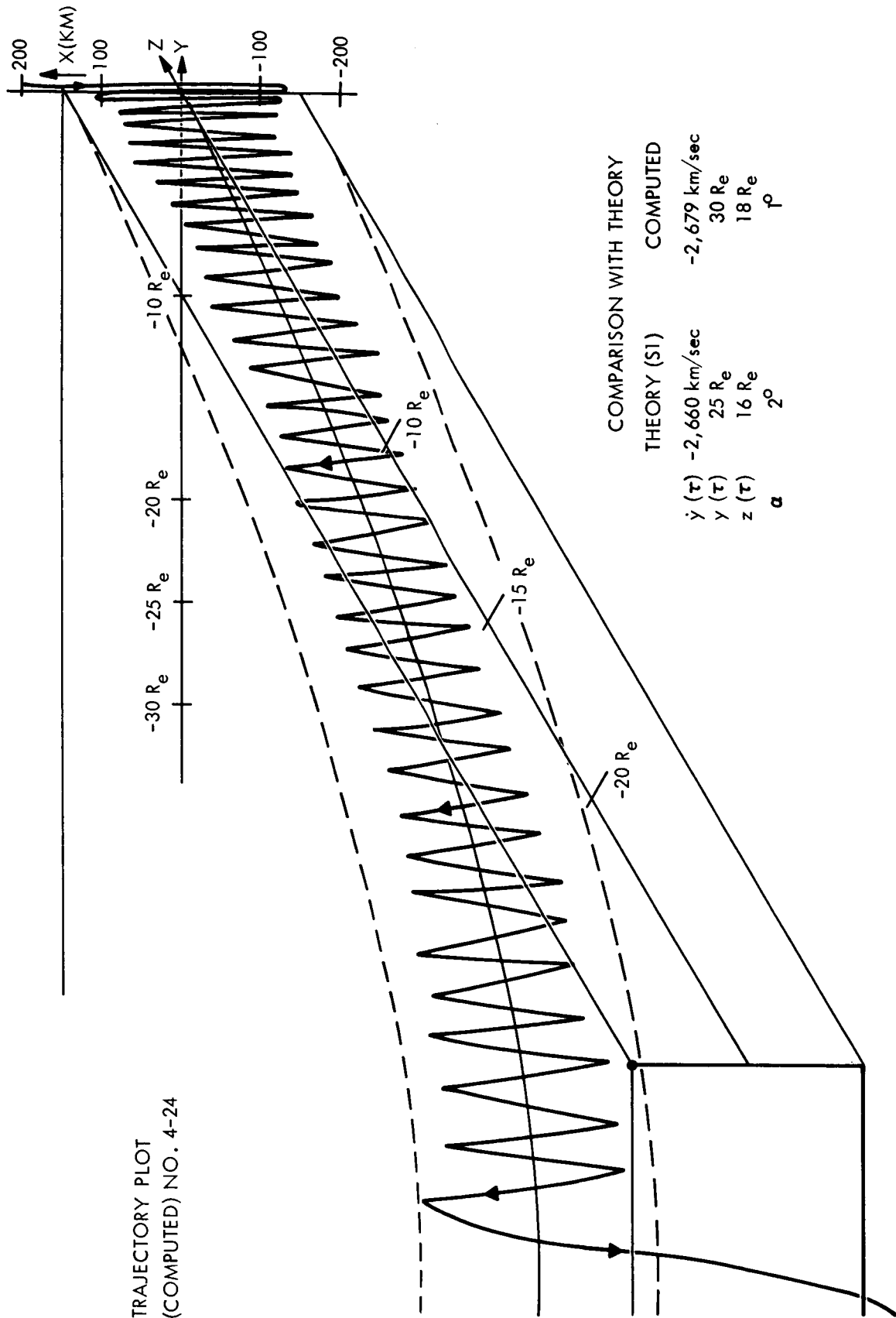
$$\vec{B}_t = \begin{cases} -b \hat{e}_y & \text{ABOVE THE SHEET} \\ -b \frac{x}{d} \hat{e}_y & \text{IN THE SHEET} \\ +b \hat{e}_y & \text{BELOW THE SHEET} \end{cases}$$

$$\vec{E} = -a \hat{e}_z$$

# PARTICLE TRAJECTORIES IN A SIMPLE NEUTRAL SHEET WITH SMALL PERPENDICULAR FIELD

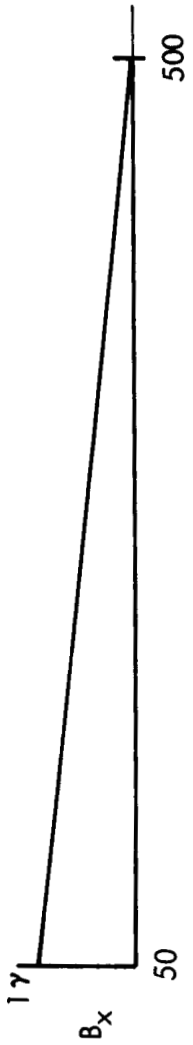
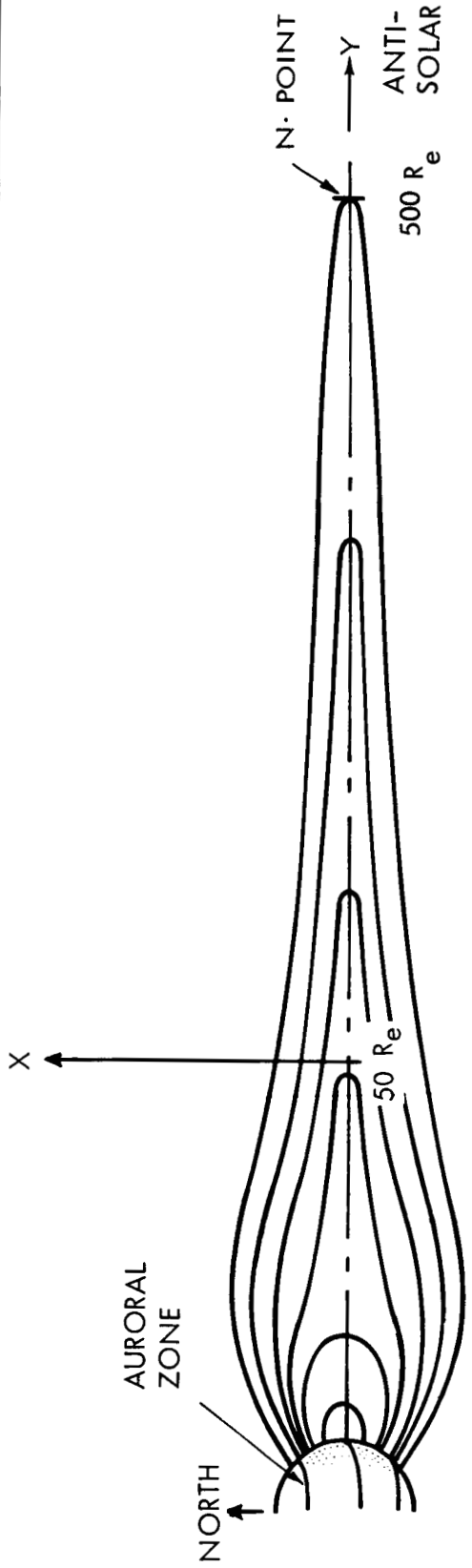


TRAJECTORY PLOT  
(COMPUTED) NO. 4-24



COMPARISON WITH THEORY

	THEORY (SI)	COMPUTED
$\dot{y}(\tau)$	-2,660 km/sec	-2,679 km/sec
$y(\tau)$	25 $R_e$	30 $R_e$
$z(\tau)$	16 $R_e$	18 $R_e$
$\alpha$	$2^\circ$	$\tau^\circ$



IN THE TAIL:

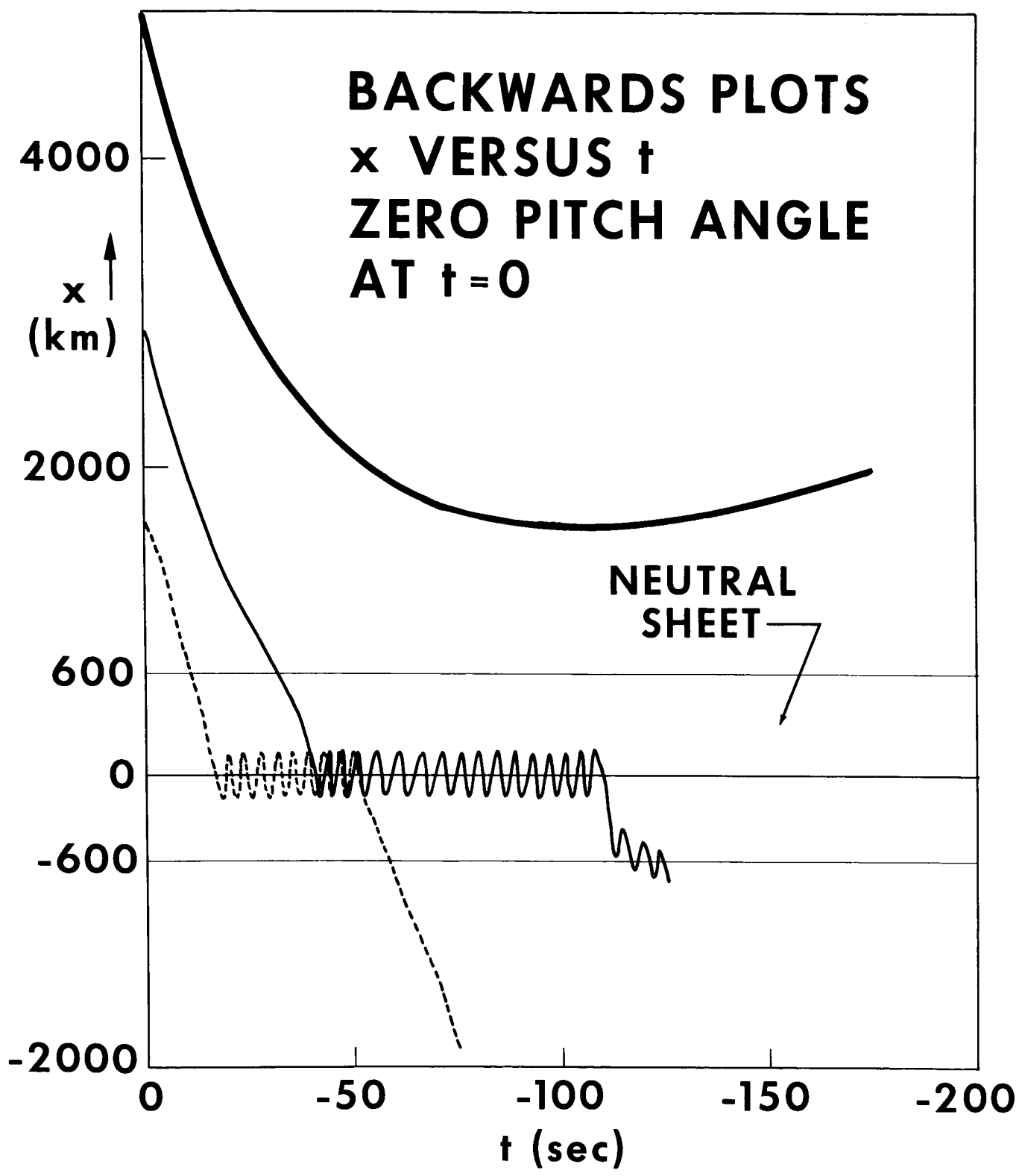
$$\underline{B} = B_x \hat{e}_x + B_y \hat{e}_y$$

$$B_y = -b \text{ ABOVE THE NEUTRAL SHEET}$$

$$B_y = -b \frac{x}{d} \text{ IN THE NEUTRAL SHEET}$$

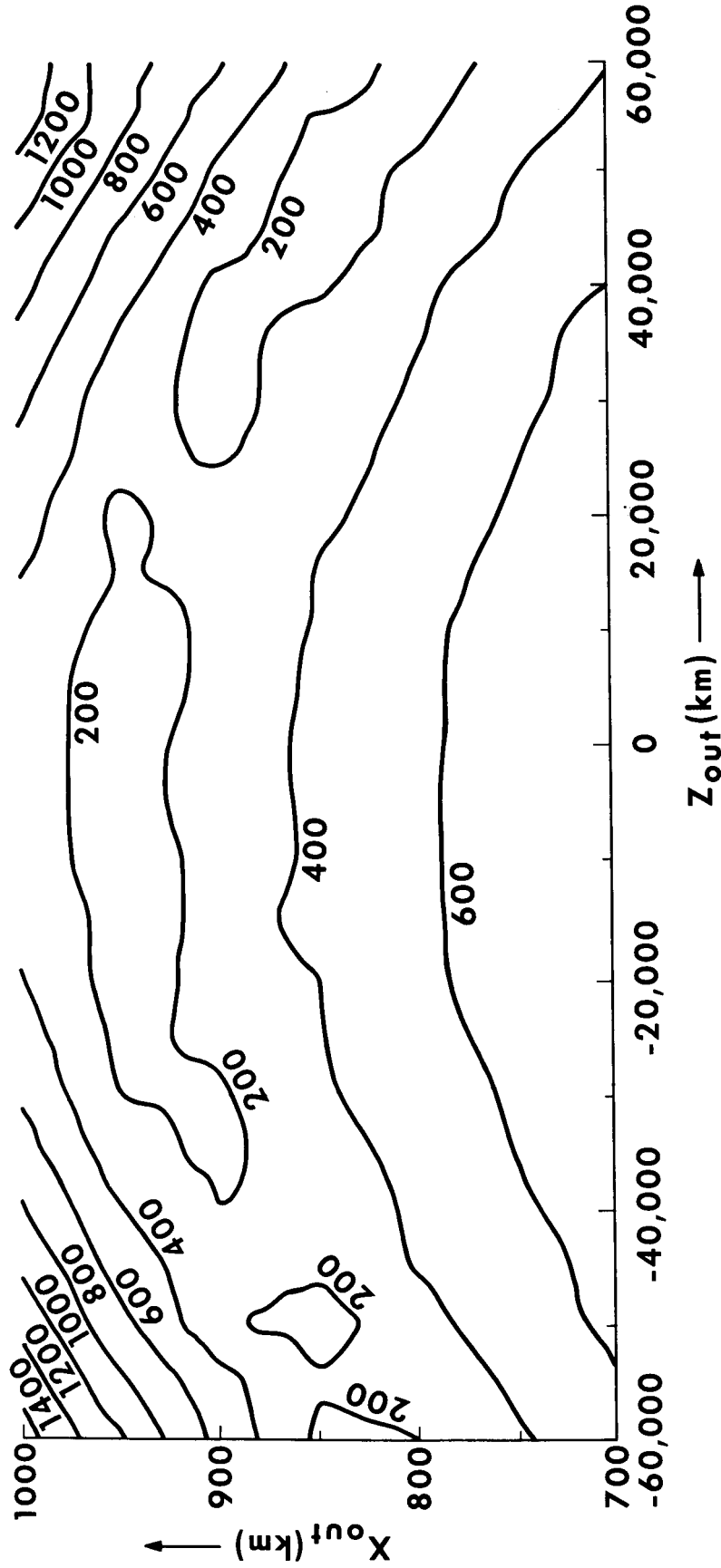
$$B_y = +b \text{ BELOW THE NEUTRAL SHEET}$$

$$\underline{E} = -\alpha \hat{e}_z$$

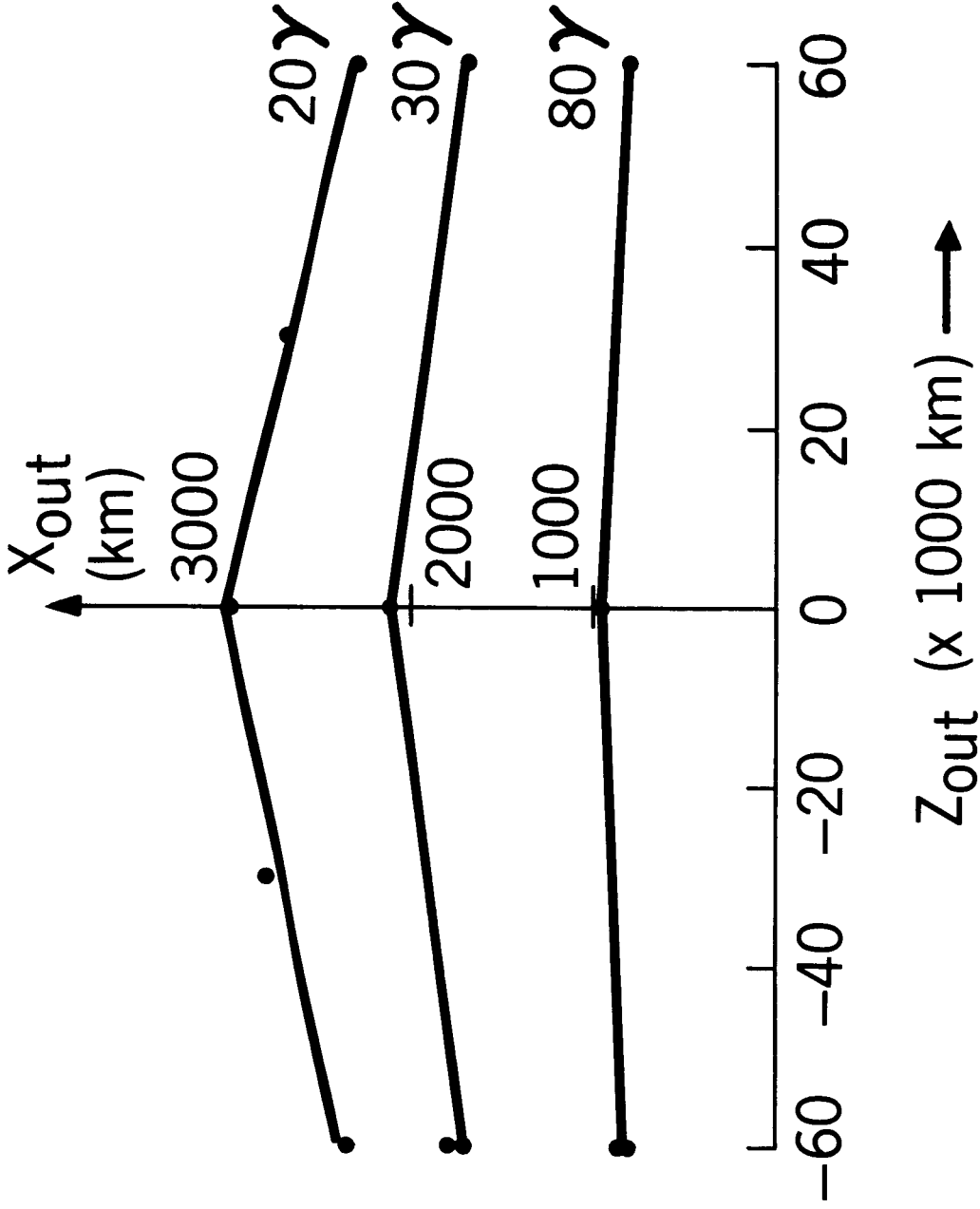


# F CONTOUR MAP ON THE $X_{OUT} - Z_{OUT}$ PLANE

$V_0 = 1664 \text{ km/sec}$ ,  $B_T = 80\gamma$



# INTERSECTION OF THE OUTPUT SHEET ( $F < V_t$ ) WITH THE $X_{out}$ - $Z_{out}$ PLANE FOR TAIL FIELDS OF $20\gamma$ , $30\gamma$ , AND $80\gamma$



# MAPPING OF OUTPUT SHEETS ONTO THE EARTH

